

Charge melting and polaron collapse in $\text{La}_{1.2}\text{Sr}_{1.8}\text{Mn}_2\text{O}_7$

L. Vasiliu-Doloc,^{1,2,*} S. Rosenkranz,³ R. Osborn,³ S. K. Sinha,³ J. W. Lynn,^{1,2} J. Mesot,³ O. H. Seeck,³ G. Preosti,^{3,4} A. J. Fedro,⁴ and J. F. Mitchell³

¹*NIST Center for Neutron Research, National Institute of Standards and Technology, Gaithersburg, Maryland 20899*

²*Department of Physics, University of Maryland, College Park, MD 20742*

³*Argonne National Laboratory, Argonne, Illinois 60439*

⁴*Department of Physics, Northern Illinois University, DeKalb, IL 60115*

X-ray and neutron scattering measurements directly demonstrate the existence of polarons in the paramagnetic phase of optimally-doped colossal magnetoresistive oxides. The polarons exhibit short-range correlations that grow with decreasing temperature, but disappear abruptly at the ferromagnetic transition because of the sudden charge delocalization. The “melting” of the charge ordering as we cool through T_C occurs with the collapse of the quasi-static polaron scattering, and provides important new insights into the relation of polarons to colossal magnetoresistance.

PACS numbers: 75.30.Vn, 75.30.Et, 71.30.+h, 71.38.+i

Manganese oxides have attracted tremendous interest because they exhibit colossal magnetoresistance (CMR) - a dramatic increase in the electrical conductivity when they order ferromagnetically. The basic relationship between ferromagnetism and conductivity in doped manganese oxides has been understood in terms of the double-exchange mechanism [1,2], where an itinerant e_g electron hops between Mn^{4+} ions, providing both the ferromagnetic exchange and electrical conduction. In addition, an important aspect of the physics of manganese oxides is the unusually strong coupling among spin, charge, and lattice degrees of freedom [2,3]. These couplings can be tuned by varying the electronic doping, electronic bandwidth, and disorder, giving rise to a complex phase diagram in which structural, magnetic, and transport properties are intimately intertwined. The charge-ordered phases represent one of the most intriguing results of balancing these couplings, and have been observed at low temperature in insulating, antiferromagnetically ordered manganites, but are incompatible with double exchange-mediated ferromagnetism seen in optimally-doped CMR systems.

In comparison to the cubic manganites such as $\text{La}_{1-x}\text{A}_x\text{MnO}_3$ (A=Sr, Ca, Ba), the two-layer Ruddlesden-Popper compounds $\text{La}_{2-2x}\text{Sr}_{1+2x}\text{Mn}_2\text{O}_7$ [4], where x is the nominal hole concentration, are advantageous to study because the reduced dimensionality strongly enhances the spin and charge fluctuations. The crystal structure is body-centered tetragonal (space group $I4/mmm$) [5] with $a \simeq 3.87$ Å and $c \simeq 20.15$ Å, and consists of MnO_2 bilayers separated by (La,Sr)O sheets. In the intermediate doping regime ($0.32 \leq x < 0.42$), the ground state is a ferromagnetic metal, and the magnetoresistance is found to be strongly enhanced near the combined metal-insulator and Curie transition at T_C (112 K for the $x=0.4$ system of present interest [6]). The present results reveal diffuse scattering associated with

lattice distortions around localized charges, i.e. polarons, in the paramagnetic phase. The formation of lattice polarons above the ferromagnetic transition temperature T_C has been inferred from a variety of measurements [7], but detailed observation via diffuse x-ray or neutron scattering in single crystals has been lacking until now [8]. Through such measurements, we have observed the collapse of quasi-static polaron scattering when the metallic, ferromagnetic state is entered. Furthermore, we present evidence of the growth of relatively well developed short-range polaron correlations in the paramagnetic phase of this optimally-doped CMR material. However, the development of long-range charge ordering is preempted by the delocalization of the polarons themselves at T_C .

The measurements were performed on a single-crystal of the double-layer compound $\text{La}_{1.2}\text{Sr}_{1.8}\text{Mn}_2\text{O}_7$, with dimensions $6 \times 4 \times 1$ mm³, cleaved from a boule that was grown using the floating-zone technique [5]. The x-ray data were taken on the 1-ID-C diffractometer at the Advanced Photon Source, mostly using a high-energy beam of 36 keV to provide enough penetration in transmission geometry. Additional measurements were taken in reflection geometry with 21 keV. The neutron measurements were performed on the BT-2 triple-axis spectrometer at the NIST research reactor, using both unpolarized (with either energy integration or energy analysis) and polarized neutron beams with an incident energy of 13.7 meV. For the measurements under magnetic field at BT-2, we employed a superconducting solenoid to provide fields up to 9 T applied in the ab plane. A wide range of reciprocal space was explored, including the $(h0l)$ and (hhl) planes.

A polaron consists of a localized charge with its associated lattice distortion field, which gives rise to diffuse scattering around the Bragg peaks, known as Huang scattering. Figure 1(a) shows a contour plot of the diffuse x-ray scattering in the $(h0l)$ plane around the $(0, 0, 8)$, $(0, 0, 10)$ and $(0, 0, 12)$ reflections [9]. A similar

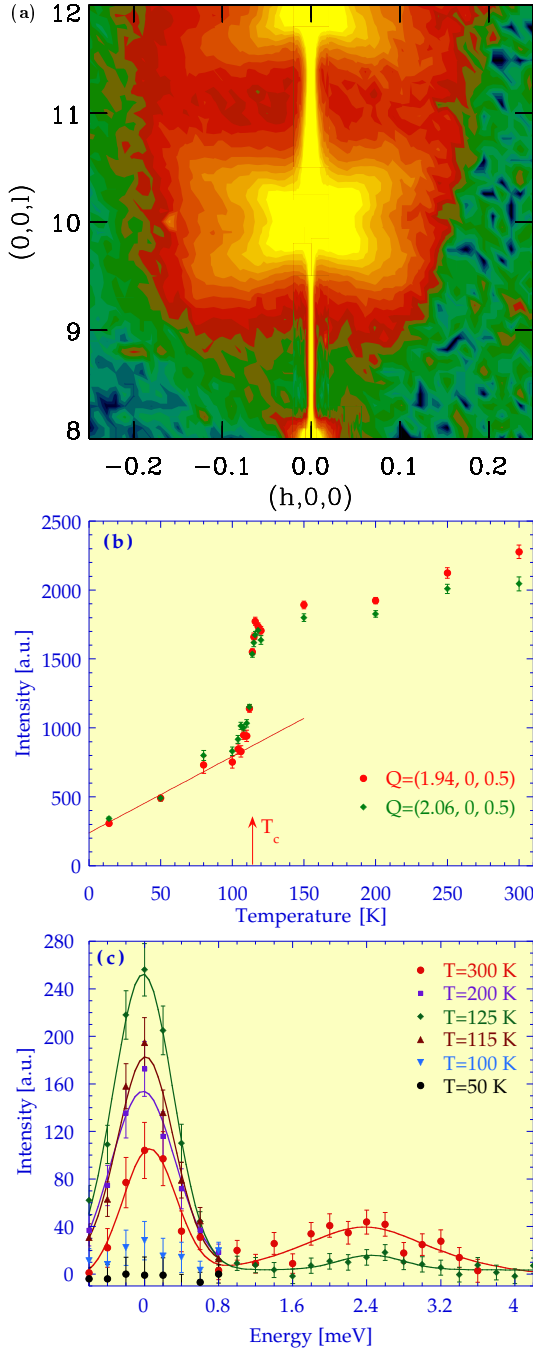


FIG. 1. (a) Contour plot showing the lobe-shaped pattern of diffuse x-ray scattering at $T=300$ K around the $(0, 0, 8)$, $(0, 0, 10)$ and $(0, 0, 12)$ reflections. (b) Observed temperature-dependence of the two $l > 0$ lobes of diffuse x-ray scattering around $(2, 0, 0)$. The straight line at low T is the estimated phonon contribution (thermal diffuse scattering), while the abrupt jump near T_C is due to the formation of polarons. (c) Neutron energy scans for several different temperatures at a wave vector $Q=(2.05, 0, 0.25)$, which is on one of the lobes of diffuse scattering around the $(2, 0, 0)$ Bragg reflection. The excitation at ~ 2.4 meV is an acoustic phonon. A flat background of 29 counts plus an elastic incoherent peak of 89 counts, measured at 10 K, have been subtracted from these data.

anisotropic pattern of diffuse scattering was observed around $(2, 0, 0)$. This scattering has a strong temperature dependence, with a dramatic response at T_C , as illustrated in Fig. 1(b). The almost linear temperature dependence of the diffuse scattering below T_C in Fig. 1(b) suggests that phonons dominate in this temperature regime [10], but the sudden change at T_C cannot be due to conventional acoustic phonons. This is confirmed by neutron energy scans such as shown in Fig. 1(c), which reveal both quasi-elastic and inelastic (phonon) contributions. The phonon mode at about 2.4 meV is well separated from the quasi-elastic scattering and obeys the usual Bose thermal population factor, whereas the quasi-elastic intensity increases with decreasing temperature, but then collapses below T_C . If we subtract an elastic nuclear incoherent contribution measured at 10 K, we see that the change at T_C is entirely due to the quasi-elastic scattering contribution, showing that the lattice distortions giving rise to it are quasi-static on a time scale $\tau \sim \hbar/2\Delta E \sim 1$ ps set by the energy resolution of the instrument, i.e. they are static on the time scale of typical phonon vibrations. A good description of the \mathbf{q} -dependence of this diffuse scattering can be obtained in terms of Huang scattering, consistent with a Jahn-Teller type distortion around the Mn^{3+} ions [11]. Our results therefore provide direct evidence both for the existence of quasi-static polarons above T_C , and their abrupt disappearance upon cooling below the ferromagnetic transition, where the charges delocalize [5,6].

The measurements also reveal the presence of broad incommensurate peaks in the paramagnetic phase, as shown by the contour plot of the x-ray intensity at 125 K in the (hk) plane at $l=18$ in Fig. 2(a). Three broad peaks are observed around the diffuse scattering rod; the expected fourth peak was not experimentally accessible. These peaks are characterized by a wave vector $(\pm\epsilon, 0, \pm 1)$ as measured from the nearest fundamental Bragg peak, where $\epsilon \simeq 0.3$ (in terms of reciprocal lattice units $(2\pi/a, 0, 2\pi/c)$). $(0, \pm\epsilon, \pm 1)$ peaks are also observed, either because of the presence of (a,b) twin domains in a $1\mathbf{q}$ -system, or because this is a $2\mathbf{q}$ -system. The in-plane incommensurability is evident in the x-ray h -scans shown in Fig. 2(b) at different temperatures. Note that, similar to the quasi-elastic peak in Fig. 1(c), this peak increases and then rapidly decreases in intensity as we cool through T_C . Figure 2(c) shows various neutron scans along the l -direction through the incommensurate peak positions $(2.3, 0, l)$. The red circles are for an energy-integrated scan that reveals two broad symmetric peaks at $l = \pm 1$, consistent with out-of-phase correlations between bilayers. Identical data are obtained in (energy integrated) x-ray scans. The orange circles depict an elastic neutron scan across one of the peaks, scaled by an instrumental factor. Energy scans at the peak positions have confirmed that the correlations giving rise to these peaks are once again quasi-static on a time scale $\tau \sim 1$ ps. We

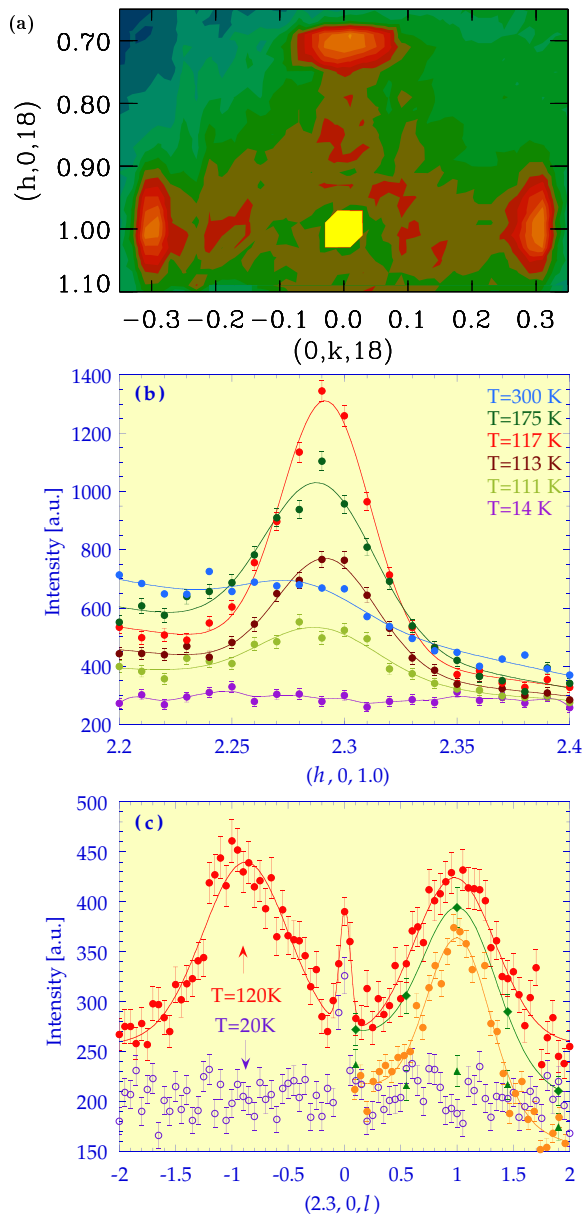


FIG. 2. Polaron ordering in $\text{La}_{1.2}\text{Sr}_{1.8}\text{Mn}_2\text{O}_7$. (a) Contour plot of the x-ray intensity in the (hk) plane at $l = 18$, collected at $T=125$ K. Three incommensurate peaks are observed, characterized by the wave vector $(\epsilon, 0, l)$ or $(0, \epsilon, l)$. The expected fourth peak was not accessible experimentally. The intensity at $(1, 0, 18)$ is due to the rod of scattering from stacking faults crossing this plane. An absorption correction based on the rotation of the sample has been applied to these data. (b) X-ray h -scans through the incommensurate peak $(2.3, 0, 1)$ at different temperatures. The higher scattering at small h is due to the proximity of the lobe-shaped diffuse scattering around the Bragg peak. (c) Neutron l -scans through the charge ordering peaks at $(2.3, 0, \pm 1)$ at $T=120$ K: energy-integrated (red), elastic (orange), non-spin-flip scattering measured with polarized neutrons (green diamonds), spin-flip scattering (green triangles). The elastic and non-spin-flip data points have been scaled by appropriate instrumental factors. The l -scan at $T=20$ K (open purple circles) shows that the charge ordering peaks have vanished.

have also performed polarized neutron experiments to probe the nature of this scattering. In the configuration where the neutron polarization $\mathbf{P} \parallel \mathbf{Q}$ (the neutron wave vector), we found that all the signal was non-spin-flip scattering (depicted by the green diamonds in Fig. 2(c)), while any magnetic scattering would be spin-flip (green triangles in Fig. 2(c)). Thus the incommensurate peaks are purely structural reflections.

Figure 3(a) shows that the temperature dependence of the incommensurate peak intensity is remarkably similar to the Huang scattering, whether the latter is derived from the x-ray scattering by subtracting the estimated thermal diffuse scattering (straight line in Fig. 1(c)) or directly from the quasi-elastic neutron scattering. This indicates that both types of scattering are associated with the development of polarons above T_C . The incommensurate peak intensity falls slightly more rapidly than the Huang scattering with increasing temperature. This is consistent with ascribing the Huang scattering to individual polarons, and the incommensurate peaks to polaron correlations which become stronger with decreasing temperature. Below T_C we observe a “melting” of the polaron correlations occurring simultaneously with the collapse of the polarons themselves. We note that the collapse of the polaron correlations also occurs under an applied magnetic field (see Fig. 3(b)). This behavior is expected because of the coupling between the charge and spin dynamics through the double exchange interaction.

The incommensurate peaks are broader than the q resolution, showing that the in-plane and out-of-plane charge correlations remain relatively short range at all temperatures. Detailed measurements in the $(h, 0, l)$ plane indicate that the correlation lengths are weakly temperature dependent and peak at the same temperature as the intensity, with $\sim 26.4 \text{ \AA} \sim 6a$ in-plane, and $\sim 10.4 \text{ \AA} \sim \frac{c}{2}$ out-of-plane. No higher harmonics have been observed, and no superlattice peaks have been found in the (hkl) plane. The $l = \pm 1$ component of the charge ordering wave vector is related to the presence of two MnO_2 bilayers per unit cell, and indicates that distortions produced by the modulation of the charge density are, on average, out of phase in adjacent bilayers. This results in a staggering of the charges from one bilayer to the next, as would be expected from Coulomb repulsion. The small c -axis correlation length (\simeq the separation between two bilayers) suggests that only two bilayers are correlated at most. The short-range nature of the charge correlations makes it difficult to collect enough integrated intensities at this stage to perform quantitative comparisons to specific charge ordering models.

Charge and orbital ordering have been observed at low temperature in a number of insulating, antiferromagnetic cubic manganites at small [12,13] and large ($x \geq 0.5$) [14] doping, as well as in layered manganites with $x=0.5$ [15]. Commensurate charge modulations in the antiferromag-

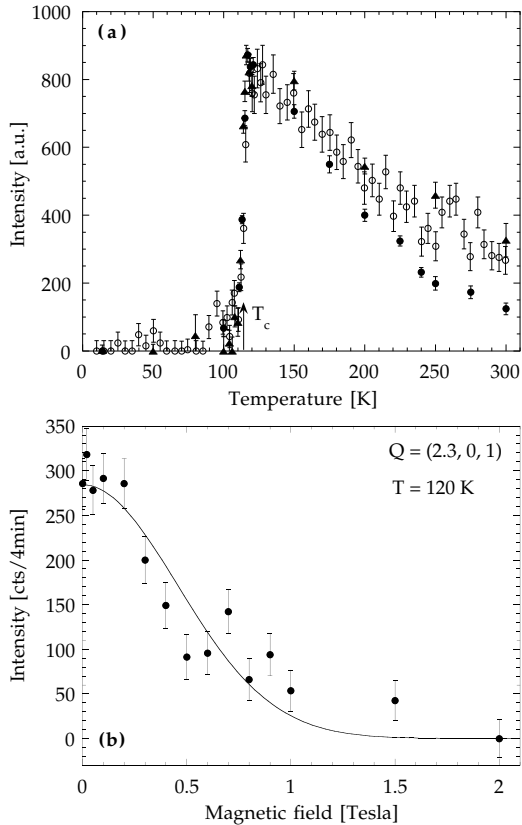


FIG. 3. (a) Temperature-dependence of the x-ray intensity of the (2.3, 0, 1) incommensurate peak (closed circles), of the diffuse x-ray scattering after correction for the phonon contribution (closed triangles), and of the quasi-elastic neutron peak (open circles) in Fig. 1(c). The diffuse scattering due to the strain field around the localized charges (polarons) and the satellite peaks due to polaron ordering collapse together at T_C . (b) Field-dependence of the intensity of the (2.3, 0, 1) peak at $T=120$ K.

netic insulating phases are also a familiar scenario in the related nickel oxides [16]. However, short-range charge ordering in the paramagnetic phase of an optimally-doped CMR ferromagnet is a novel feature observed here. The charge correlations result from Coulomb interactions between the polarons, coupled with the interaction of overlapping polaronic strain fields. In the present $x=0.4$ system they are not strong enough to win the competition with the double exchange interaction, and the charges delocalize at the ferromagnetic transition, where the charge peaks collapse and the lattice strain relaxes. It is the delicate balance between double exchange, Coulomb repulsion and the lattice strain field that dictates whether the material is a ferromagnetic metal or charge-ordered insulator at low temperatures.

This work was supported by the U.S. Department of Energy, Basic Energy Sciences-Materials Sciences (W-31-109-ENG-38), NSF (DMR 97-01339), NSF-MRSEC (DMR 96-32521), and the Swiss National Science Foundation. We are grateful to N. Wakabayashi for drawing

our attention to similar x-ray diffuse scattering observations [8], and to W.-K. Lee for his help with the x-ray measurements.

* Present address: Department of Physics, Northern Illinois University, DeKalb, IL 60115, and Argonne National Laboratory, Argonne, IL 60439.

- [1] C. Zener, Phys. Rev. **82**, 403 (1951); J. B. Goodenough, Phys. Rev. **100**, 564 (1955).
- [2] For a recent review, see A. Moreo, S. Yunoki, and E. Dagotto, Science **283**, 2034 (1999).
- [3] See, for example, A. J. Millis, P. B. Littlewood, and B. I. Shraiman, Phys. Rev. Lett. **74**, 5144 (1995); H. Röder, J. Zang, and A. R. Bishop, Phys. Rev. Lett. **76**, 1356 (1996); A. J. Millis, Phys. Rev. B **53**, 8434 (1996); A. S. Alexandrov and A. M. Bratkovsky, Phys. Rev. Lett. **82**, 141 (1999); C. M. Varma, Phys. Rev. B **54**, 7328 (1996).
- [4] Y. Moritomo, A. Asamitsu, H. Kuwahara, and Y. Tokura, Nature (London) **380**, 141 (1996).
- [5] J. F. Mitchell, D. N. Argyriou, J. D. Jorgensen, D. G. Hinks, C. D. Potter, and S. D. Bader, Phys. Rev. B **55**, 63 (1997).
- [6] R. Osborn, S. Rosenkranz, D. N. Argyriou, L. Vasiliu-Doloc, J. W. Lynn, S. K. Sinha, J. F. Mitchell, K. E. Gray, and S. D. Bader, Phys. Rev. Lett. **81**, 3964 (1998).
- [7] S. J. L. Billinge, R. G. DiFrancesco, G. H. Kwei, J. J. Neumeier, and J. D. Thompson, Phys. Rev. Lett. **77**, 715 (1996); D. Louca, T. Egami, E. L. Brosha, H. Röder, and A. R. Bishop, Phys. Rev. B **56**, R8475, 1997. For a review, see A. S. Alexandrov and N. F. Mott, *Polarons and Bipolarons* (World Scientific, Singapore, 1995).
- [8] We were recently made aware of similar observations of x-ray diffuse scattering in a perovskite compound by S. Shimomura, N. Wakabayashi, H. Kuwahara, and Y. Tokura. Their conclusions are very similar to our own.
- [9] The sharp rod of scattering along the $[0, 0, l]$ direction is resolution limited in the $(hk0)$ plane and is associated with stacking faults inevitably found in crystals with layered structures.
- [10] Such diffuse scattering patterns have also been seen in doped lanthanum nickelates and cuprates, but with a conventional temperature dependence; E. D. Isaacs, G. Aeppli, P. Zschack, S.-W. Cheong, H. Williams, and D. J. Buttrey, Phys. Rev. Lett. **72**, 3421 (1994).
- [11] G. Preosti et al., preprint.
- [12] Y. Murakami, J. P. Hill, D. Gibbs, M. Blume, I. Koyama, M. Tanaka, H. Kawata, T. Arima, Y. Tokura, K. Hirota, and Y. Endoh, Phys. Rev. Lett. **81**, 582 (1998).
- [13] Y. Endoh, K. Hirota, S. Ishihara, S. Okamoto, Y. Murakami, A. Nishizawa, T. Fukuda, H. Kimura, H. Nojiri, K. Kaneko, and S. Maekawa, Phys. Rev. Lett. **82**, 4328 (1999).
- [14] S. Mori, C. H. Chen, and S.-W. Cheong, Nature (London) **392**, 473 (1998); S. Mori, C. H. Chen, and S.-W. Cheong, Phys. Rev. Lett. **81**, 3972 (1998).
- [15] J. Q. Li, Y. Matsui, T. Kimura, and Y. Tokura, Phys. Rev. B **57**, R3205 (1998).
- [16] C. H. Chen, S.-W. Cheong, and A. S. Cooper, Phys. Rev. Lett. **71**, 2461 (1993).